Hindawi
Journal of Nanomaterials
Volume 2018, Article ID 7074824, 6 pages
https://doi.org/10.1155/2018/7074824

Research Article

High Rate Performance of Ca-Doped $Li_4Ti_5O_{12}$ Anode Nanomaterial for the Lithium-Ion Batteries

Heming Deng,[1] **Wei Liang**,[1] **Dexin Nie**,[1] **Jian Wang**,[2] **Xu Gao**,[1] **Shun Tang**,[3] **Cui Liu**,[3] **and Yuan-Cheng Cao**[4]

[1]*State Grid Electric Power Research Institute, Wuhan, China 430074*
[2]*State Grid Xinjiang Electric Power Company, Urumqi, China 830011*
[3]*Key Lab of Optoelectronic Chemical Materials and Devices, Ministry of Education, Jianghan University, Wuhan 430056, China*
[4]*State Key Laboratory of Advanced Electromagnetic Engineering and Technology, School of Electrical and Electronic Engineering, Huazhong University of Science and Technology, Wuhan 430074, China*

Correspondence should be addressed to Heming Deng; dengheming@sgepri.sgcc.com.cn
and Shun Tang; shun.tang.2010@hotmail.com

Received 21 May 2018; Accepted 1 August 2018; Published 17 September 2018

Academic Editor: Victor M. Castaño

The spinel $Li_4Ti_5O_{12}$ (LTO) has been doped by Ca^{2+} via a solid-state reaction route, generating highly crystalline $Li_{3.9}Ca_{0.1}Ti_5O_{12}$ powders in order to improve the electrochemical performance as an anode. The structure changes, morphologies, and electrochemical properties of the resultant powders have been characterized by X-ray diffraction (XRD), scanning electron microscopy (SEM), and cyclic voltammetry (CV), respectively. Crystal structure and composition were analyzed, and results were obtained with various tests of LTO. Electrochemical measurements revealed that $Li_{3.9}Ca_{0.1}Ti_5O_{12}$ anodes exhibit better rate capability, better cycling stability, and a higher specific capacity than pure LTO anodes.

1. Introduction

Lithium-ion batteries (LIBs) have been widely utilized as the most important next-generation energy sources [1, 2]. However, the carbon anode materials are facing safety issues caused by relatively low Li-intercalation potential (about 0 V vs. Li/Li^+). As an alternative anode material for LIBs, spinel $Li_4Ti_5O_{12}$ (LTO) has attracted more and more attention because of its extremely small volume change during Li^+ insertion/extraction as the so-called "zero strain material" [3]. At the same time, LTO possesses the fast Li^+ insertion and deinsertion ability, excellent cycle stability, and high thermal stability due to its voltage plateau at 1.55 V (vs. Li/Li^+), which can inhibit the decomposition of the electrolyte on the electrode/electrolyte surface and hence reinforce the safety of LIBs [4]. Unfortunately, LTO exhibits a poor electronic conductivity [5]. To improve the conductivity, a considerable number of effective ways have been developed. Generally, the strategy includes the preparation of nanometer particles [6], carbon coating [7], and doping with aliovalent metal ions [8–15] (V^{5+} [8], Sr^{2+} [9], La^{3+} [10], Mg^{2+} [11], Al^{3+} [12], Co^{3+} [13], and Ru^{3+} [14]) in Li, Ti, or O sites; the selection of morphologies has a crucial influence on the electrochemical characteristics of LTO materials [15–18]. Additionally, there are literatures which reported various strategies including combined ion coping or sheet-encapsulated coating [12, 19–22]. In this work, the effects of Ca-doping on the microstructure, morphology, and electrochemical characteristics of LTO have been investigated. The doped Ca^{2+} can replace the Li^+ of 8a to produce free electrons, thus enhancing the conductivity of the material. The results indicate that the Ca-doped LTO ($Li_{3.9}Ca_{0.1}Ti_5O_{12}$) delivers a large capacity at a high rate with excellent cycle performance, which provides a potential technique for the application of LTO in LIBs with high performance.

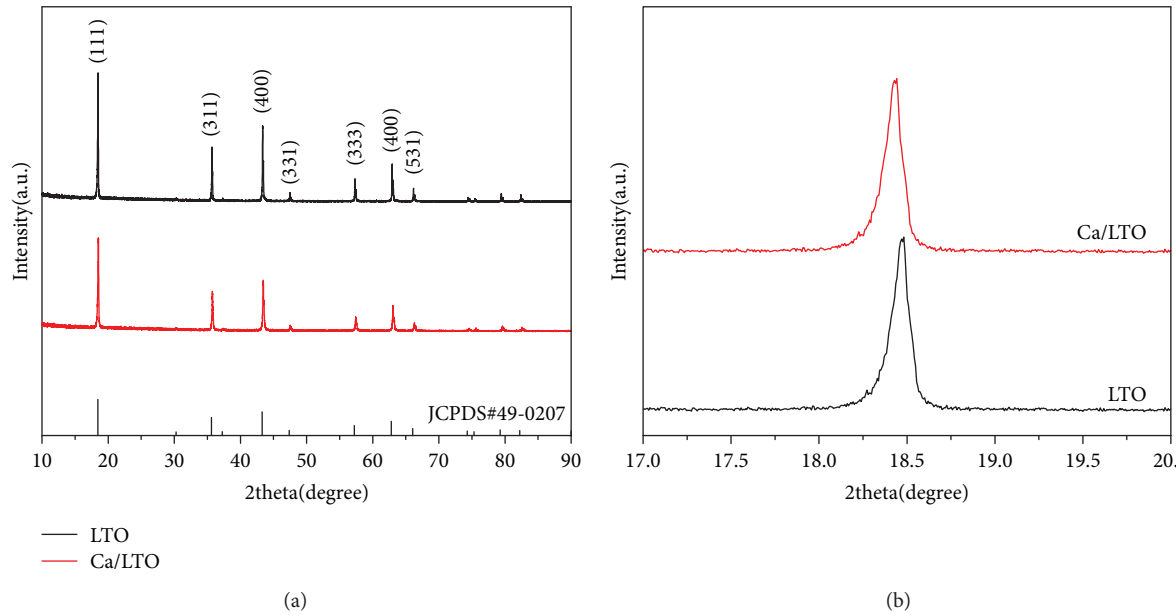

Figure 1: XRD patterns of the $Li_4Ti_5O_{12}$ and the $Li_{3.9}Ca_{0.1}Ti_5O_{12}$ (a) and enlarged (111) peaks (b) of $Li_4Ti_5O_{12}$ and $Li_{3.9}Ca_{0.1}Ti_5O_{12}$.

2. Materials and Methods

2.1. Preparation of the Samples. Ca-doped LTO ($Li_{3.9}Ca_{0.1}Ti_5O_{12}$) and undoped $Li_4Ti_5O_{12}$ were generated via solid-state reaction route. CaO was used as a calcium source for doping. Excess Li (2 wt%) was necessary because of the loss of Li during synthesis at high temperature. A mixture of TiO_2, Li_2CO_3, and CaO in a proper amount in high-energy ball milling for half an hour; then, the powders were put in a continuous heating tube furnace at 800°C for 12 h in a flowing Ar atmosphere.

2.2. Preparation of the Batteries. In order to prepare the electrode, LTO or Ca-doped LTO, super carbon, and polyvinylidene fluoride (PVDF) (LTO/C/PVDF in a weight ratio of 8 : 1 : 1) were uniformly mixed in N-methyl pyrrolidone (NMP) solvent to produce homogeneous slurry, which was cast on a copper foil by a blade. The solvent was evaporated under vacuum at 110°C overnight. The electrode was punched to a disk shape with a diameter of 16 mm. Half cells were assembled in a glove box with metallic lithium foils as the counter electrode, microporous polyethylene membranes (Celgard 2400) as the separators, and 1 M $LiPF_6$ in a mixture of ethyl carbonate (EC) and dimethyl carbonate (DMC) (EC/DMC in a volume ratio of 1 : 1) as the electrolyte [19–22].

2.3. Material Characterization. The structure and morphology of the Ca-doped LTO powders were characterized by X-ray diffraction measurement (XRD, PANalytical, X'Pert Powder) and scanning electron microscopy (SEM, Hitachi, SU8010). Galvanostatic cycling was conducted on a Wuhan LAND Electronics Battery Tester. Cyclic voltammetry (CV) was tested on an electrochemical workstation (Autolab, PASTAT101) between 0.8 and 2.8 V (vs. Li^+/Li) at a scanning rate of 0.5 mV s^{-1}. Electrochemical impedance spectrum (EIS) measurements were also tested using Autolab at a potentiostatic signal amplitude of 5 mV and with a frequency range from 10 MHz to 1 MHz [23].

3. Results and Discussions

XRD patterns of the obtained LTO and Ca-doped LTO are shown in Figure 1(a). The diffraction peaks of all the samples can be completely indexed in the cubic spinel structure (JCPDS#49-0207). No impurity peaks were observed, which indicates that the Ca has entered the lattice structure of LTO without changing its crystal structures. And also, it is hypothesized that the narrow width of the Ca-doped LTO peaks is caused by the high crystallinity of the powders [24].

For clear observation, enlarged (111) peaks of LTO and $Li_{3.9}Ca_{0.1}Ti_5O_{12}$ are shown in Figure 1(b). It can be observed that the (111) peak shifted to low angle with Ca-doping, suggesting that the doped LTO samples possess larger lattice constant than pristine LTO. This result could be attributed to Ca-doping which makes the phase structure change from a cubic structure to an oblique crystal structure and opens up a channel favorable for lithium-ion migration along the *b* axis. The substitution of Li^+ with the valence of Li^+ is the formation of Ti^{4+}/Ti^{3+}-mixed valence state at B site based on charge compensation. As a result, the lattice constant was only slightly enlarged. Theoretically, the lattice stability could be maintained during the fast lithium-ion transfer, which would improve the performance of Ca-doped LTO electrodes in cell testing.

SEM images of LTO powders with and without Ca-doping are illustrated, respectively, in Figure 2. Both of the two materials possess uniform particle size distribution. Generally, the crystallite size is ranged from 100 to 200 nm in both samples. This fine microstructure could be attributed to the well dispersion and fully reaction of TiO_2, Li_2CO_3, and CaO. It can be explained that the small particle size is beneficial for decreasing the interface impedance between

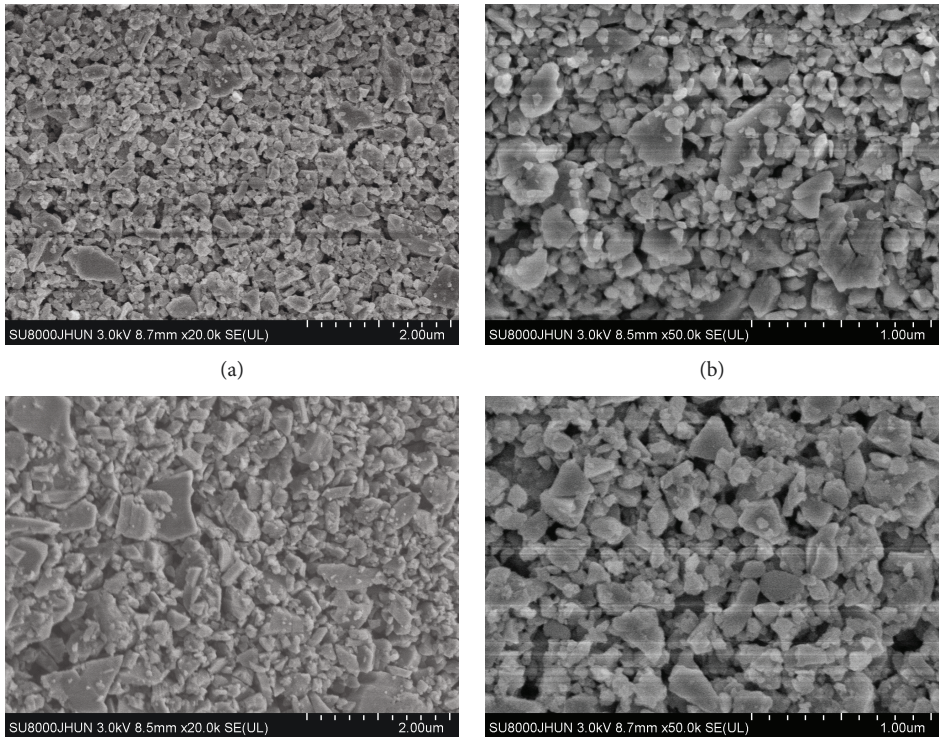

Figure 2: SEM images of $Li_{3.9}Ca_{0.1}Ti_5O_{12}$ (a, b) and $Li_4Ti_5O_{12}$ (c, d).

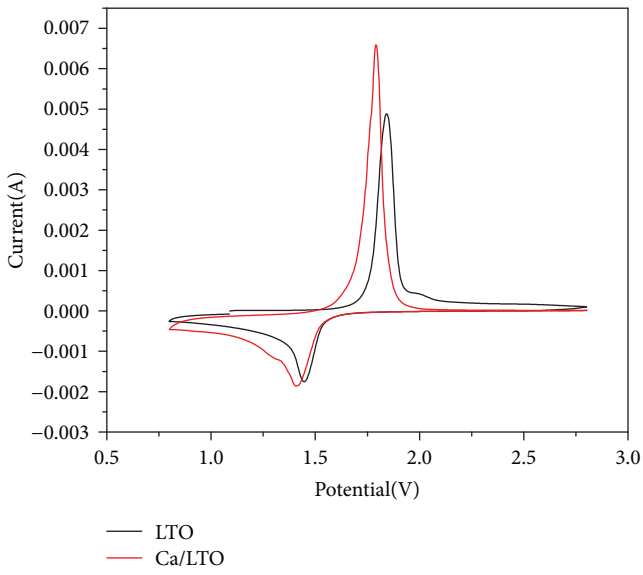

Figure 3: Cyclic voltammetry potentiostatic of LTO and $Li_{3.9}Ca_{0.1}Ti_5O_{12}$ (Ca/LTO) (0.8–2.8 V, 0.5 mV/s).

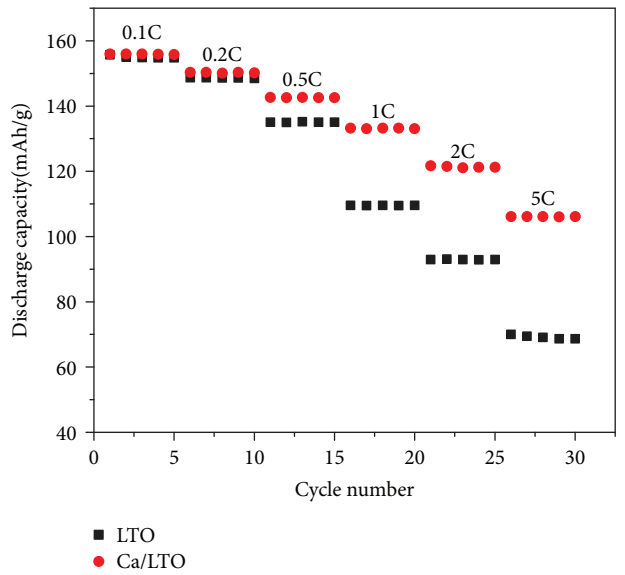

Figure 4: The rate capability measurements of the $L_4Ti_5O_{12}$ (LTO) and $Li_{3.9}Ca_{0.1}Ti_5O_{12}$ (Ca/LTO) samples at different cycling rates.

the active materials and electrolytes which thus promotes the efficiency of Li^+ insertion/extraction into the LTO crystal structure [25].

In order to investigate the effect of Ca-doping on improving electrochemical properties, cyclic voltammetry potentiostatic (CV) of $Li_{3.9}Ca_{0.1}Ti_5O_{12}$ and LTO electrodes have been measured at a scan rate of 0.5 mV s^{-1} between 0.8 V and 2.8 V (Figure 3). It is obvious that there is a pair of reversible redox peaks for each sample, which represents the lithium insertion process (reduction peaks at about 1.50 V vs. Li^+/Li) and extraction process (oxidation peaks at about 1.75 V vs. Li^+/Li). It is attributed to the typical two-phase reaction of the redox couple of Ti^{3+}/Ti^{4+} during Li^+ insertion/extraction processes. The corresponding electrochemical reaction is $Li_4Ti_5O_{12} + 3Li^+ + 3e - \rightarrow Li_7Ti_5O_{12}$ ($E = 1.55$ V) [26].

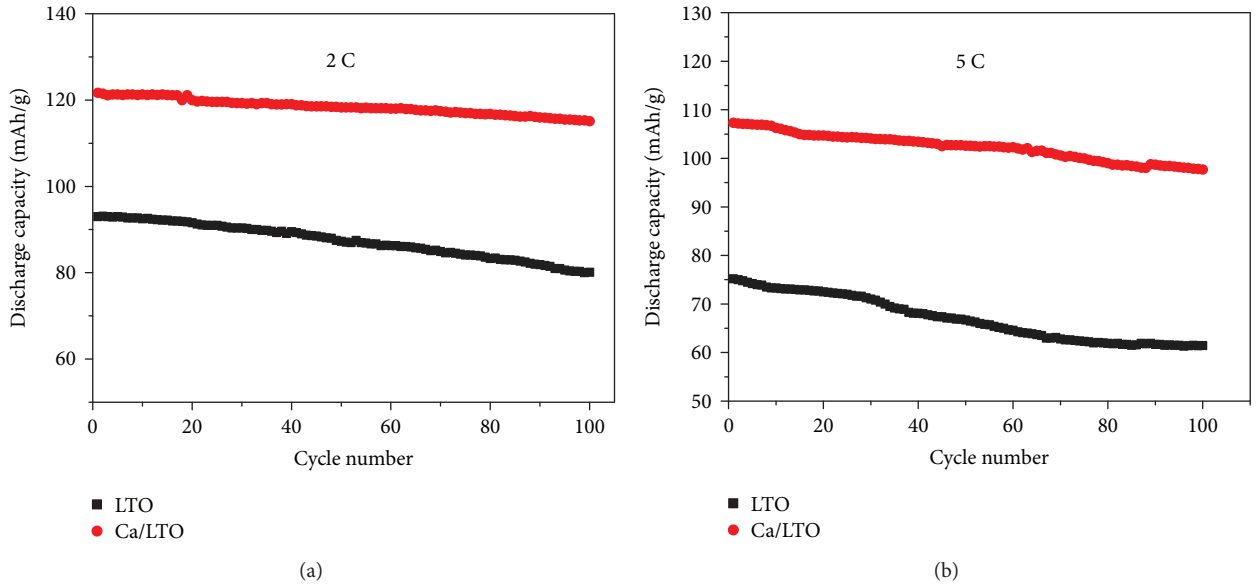

Figure 5: Cycling performance of $Li_4Ti_5O_{12}$ (LTO) and $Li_{3.9}Ca_{0.1}Ti_5O_{12}$ (Ca/LTO) samples at 2C (a) and 5C (b) rates.

The rate capability of the Ca/LTO and LTO electrodes at different rates is presented in Figure 4. It can be observed that the Ca-doped LTO exhibited a higher discharge capacity and good cycling stability at a low rate, and its initial discharge capacity could reach up to 155.7 mAh g^{-1} when at 0.1C. As the discharge rate increases, the capacity of undoped LTO quickly decreases. However, the Ca-doped LTO exhibits less capacity degradation. At 5C, the discharge specific capacity of LTO and Ca/LTO was 68.7 mAh g^{-1} and 106.1 mAh g^{-1}, respectively. Compared with the first discharge capacity, the retention rate was 44.12% and 68.01%, respectively. The better rate capability and cycling stability of Ca-doped LTO were observed because of the efficient Li^+ insertion/extraction induced by Ca-doping.

The cycling performance of the LTO and Ca/LTO samples at rates of 2C and 5C is shown in Figure 5. As expected, Ca/LTO electrodes exhibited higher reversible capacities than that of undoped LTO. At 2C, the discharge capacity of Ca/LTO remained 115.1 mAh g^{-1} even after 100 cycles (Figure 5(a)). Compared with the first discharge specific capacity of 121.7 mAh g^{-1}, the attenuation amplitude was only 5.42%. In contrast, the corresponding value of the LTO was decreased to 80.1 mAh g^{-1}. The attenuation was 13.87%. When at 5C rate (Figure 5(b)), the initial discharge capacity of Ca/LTO was 107.3 mAh g^{-1} and remained as high as 97.7 mAh g^{-1} after 100 cycles (91.05% retention), while the initial discharge capacity of LTO was 75.2 mAh g^{-1} and remained 61.4 mAh g^{-1} after 100 cycles. These results demonstrate that the Li^+ insertion/extraction processes of Ca/LTO exhibits better reversibility and cyclic stability even at high rates and higher capacity retention than pure LTO, which should be attributed to the relatively slight change of lattice volume in Ca-doped LTO electrodes during the insertion and extraction of Li^+.

To evaluate the electrochemical performance of Ca-doped LTO electrodes in LIBs, galvanostatic charge-discharge tests have been carried out. Figure 6 shows the initial charge-discharge curves of the LTO and Ca/LTO samples at various current rates from 0.1C to 5C [27]. It is obvious that the discharge plateau of each material decreases with increasing current rate, because of the increased polarization of electrodes. The Ca/LTO delivered relatively higher discharge-specific capacities especially at high current rates.

Figure 7 shows the EIS curves of cells with LTO and Ca/LTO at the voltage of 1.55 V after 20 cycles. The Ca/LTO electrode exhibits relatively lower resistance than pure LTO electrode, which is consistent with the result of the better reversible capacities. In the EIS patterns, a semicircle in the high-frequency region and a straight line in the low-frequency region are observed. The semicircle is related to the charge transfer resistance between the active material interface and the electrolyte, while the straight line represents the Warburg impedance that is related to diffusion of Li^+ [28–30]. In the equivalent circuit, W is the Warburg impedance, and R_s and R_{ct} represent the ohmic resistance and the charge transfer resistance, respectively [20–32]. The diffusion coefficient values of the lithium ions in the bulk electrode materials were calculated from EIS data demonstrating that the charge transfer process of Li^+ on the surface of Ca/LTO electrodes has been significantly improved and ion conductivity of Ca/LTO electrodes has been promoted via Ca-doping.

4. Conclusions

Generally, the Ca-doped LTO can be synthesized by solid-state methods and the electrochemical performance of Ca-doped LTO is much better than the pure LTO. There was no significant change in the particle morphology of LTO powders after Ca-doping, and the small particle size is beneficial for decreasing the interface impedance between the active materials and electrolytes which thus promotes the efficiency of Li^+ insertion/extraction into the LTO crystal

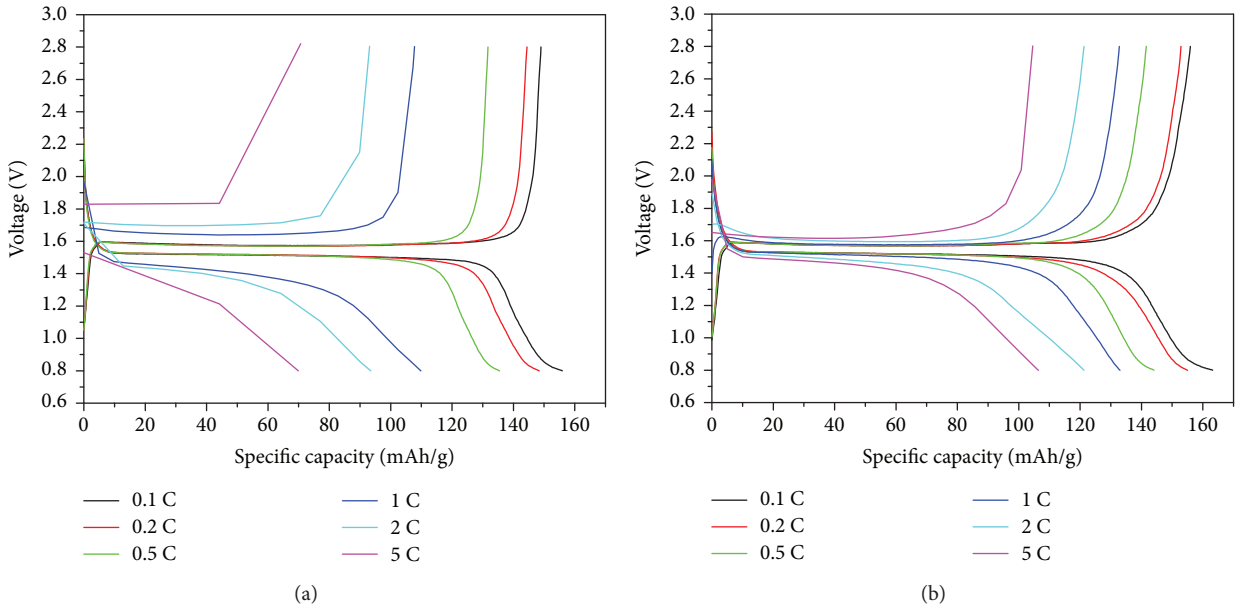

Figure 6: Initial charged-discharged performance of $L_4Ti_5O_{12}$ (a) and $Li_{3.9}Ca_{0.1}Ti_5O_{12}$ (b) at various rates.

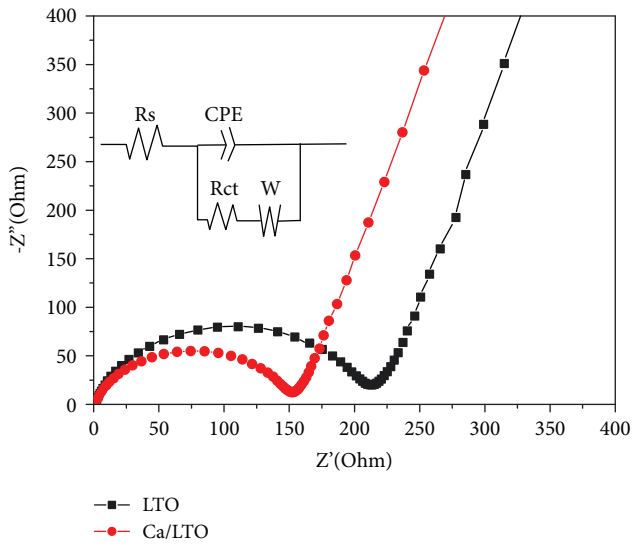

Figure 7: The EIS plots of the AC impedance for the $Li_4Ti_5O_{12}$ (LTO) and $Li_{3.9}Ca_{0.1}Ti_5O_{12}$.

structure. The rate capability, cyclic stability, and the ion conductivity of the half cells with Ca-doped LTO anodes have been significantly improved, compared to cells assembled with the pure LTO, which should be attributed to the relatively slight change of lattice volume in Ca-doped LTO electrodes during the insertion and extraction of Li^+. The excellent performance of Ca-doped LTO anodes can be attributed to its promoted charge transfer of Li^+ and relatively lower interfacial resistance arising from Ca-doping. The Ca/LTO delivers relatively higher discharge-specific capacities especially at high current rates. The charge transfer process of Li^+ on the surface of Ca/LTO electrodes can be significantly improved, and ion conductivity of Ca/LTO electrodes has been promoted via Ca-doping. All the results demonstrate that the Ca-doped LTO materials could be potential in the application of safe LTO anodes in high rate LIBs.

Data Availability

The data used to support the findings of this study are available from the corresponding author upon request.

Conflicts of Interest

The authors declare no conflict of interest.

Acknowledgments

This project was supported by the fund from China NSF (51703081), Wuhan Applied Basic Research Project (2018010401011285), and 4th Yellow Crane Talent Programme of Wuhan City (08010004).

References

[1] W. Wang, B. Jiang, W. Xiong, Z. Wang, and S. Jiao, "A nanoparticle Mg-doped $Li_4Ti_5O_{12}$ for high rate lithium-ion batteries," *Electrochimica Acta*, vol. 114, pp. 198–204, 2013.

[2] L. Xu, S. Tang, Y. Cheng et al., "Interfaces in solid-state lithium batteries," *Joule*, 2018.

[3] J.-G. Kim, D. Shi, M.-S. Park et al., "Controlled Ag-driven superior rate-capability of $Li_4Ti_5O_{12}$ anodes for lithium rechargeable batteries," *Nano Research*, vol. 6, no. 5, pp. 365–372, 2013.

[4] Q. Zhang, C. Zhang, B. Li et al., "Preparation and characterization of W-doped $Li_4Ti_5O_{12}$ anode material for enhancing the high rate performance," *Electrochimica Acta*, vol. 107, pp. 139–146, 2013.

[5] S. Ji, J. Zhang, W. Wang et al., "Preparation and effects of Mg-doping on the electrochemical properties of spinel $Li_4Ti_5O_{12}$ as anode material for lithium ion battery," *Materials Chemistry and Physics*, vol. 123, no. 2-3, pp. 510–515, 2010.

[6] J. Cheng, R. Che, C. Liang, J. Liu, M. Wang, and J. Xu, "Hierarchical hollow $Li_4Ti_5O_{12}$ urchin-like microspheres with ultra-high specific surface area for high rate lithium ion batteries," *Nano Research*, vol. 7, no. 7, pp. 1043–1053, 2014.

[7] Q. Cheng, S. Tang, C. Liu et al., "Preparation of carbon encapsulated $Li_4Ti_5O_{12}$ anode material for lithium ion battery through pre-coating method," *Ionics*, vol. 23, no. 11, pp. 3031–3036, 2017.

[8] Z. Yu, X. Zhang, G. Yang et al., "High rate capability and long-term cyclability of $Li_4Ti_{4.9}V_{0.1}O_{12}$ as anode material in lithium ion battery," *Electrochimica Acta*, vol. 56, no. 24, pp. 8611–8617, 2011.

[9] H. Wu, S. Chang, X. Liu et al., "Sr-doped $Li_4Ti_5O_{12}$ as the anode material for lithium-ion batteries," *Solid State Ionics*, vol. 232, pp. 13–18, 2013.

[10] D. Wang, C. Zhang, Y. Zhang, J. Wang, and D. He, "Synthesis and electrochemical properties of La-doped $Li_4Ti_5O_{12}$ as anode material for Li-ion battery," *Ceramics International*, vol. 39, no. 5, pp. 5145–5149, 2013.

[11] Q. Cheng, S. Tang, C. Liu et al., "Preparation and electrochemical performance of $Li_{4-x}Mg_xTi_5O_{12}$ as anode materials for lithium-ion battery," *Journal of Alloys and Compounds*, vol. 722, pp. 229–234, 2017.

[12] M. Krajewski, B. Hamankiewicz, M. Michalska, M. Andrzejczuk, L. Lipinska, and A. Czerwinski, "Electrochemical properties of lithium–titanium oxide, modified with Ag–Cu particles, as a negative electrode for lithium-ion batteries," *RSC Advances*, vol. 7, no. 82, pp. 52151–52164, 2017.

[13] C. Zhang, D. Shao, J. Yu et al., "Synthesis and electrochemical performance of cubic Co-doped $Li_4Ti_5O_{12}$ anode material for high-performance lithium-ion batteries," *Journal of Electroanalytical Chemistry*, vol. 776, pp. 188–192, 2016.

[14] W. Wang, H. Wang, S. Wang, Y. Hu, Q. Tian, and S. Jiao, "Ru-doped $Li_4Ti_5O_{12}$ anode materials for high rate lithium-ion batteries," *Journal of Power Sources*, vol. 228, pp. 244–249, 2013.

[15] G. N. Zhu, H. J. Liu, J. H. Zhuang, C. X. Wang, Y. G. Wang, and Y. Y. Xia, "Carbon-coated nano-sized $Li_4Ti_5O_{12}$ nanoporous micro-sphere as anode material for high-rate lithium-ion batteries," *Energy & Environmental Science*, vol. 4, no. 10, p. 4016, 2011.

[16] J. Wang, F. Zhao, J. Cao, Y. Liu, and B. Wang, "Enhanced electrochemical performance of Cu_2O-modified $Li_4Ti_5O_{12}$ anode material for lithium-ion batteries," *Ionics*, vol. 21, no. 8, pp. 2155–2160, 2015.

[17] L. Shen, X. Zhang, E. Uchaker, C. Yuan, and G. Cao, "$Li_4Ti_5O_{12}$ nanoparticles embedded in a mesoporous carbon matrix as a superior anode material for high rate lithium ion batteries," *Advanced Energy Materials*, vol. 2, no. 6, pp. 691–698, 2012.

[18] J. Jiang, P. Nie, B. Ding et al., "Effect of graphene modified Cu current collector on the performance of $Li_4Ti_5O_{12}$ anode for lithium-ion batteries," *ACS Applied Materials & Interfaces*, vol. 8, no. 45, pp. 30926–30932, 2016.

[19] C. Lin, B. Ding, Y. Xin et al., "Advanced electrochemical performance of $Li_4Ti_5O_{12}$-based materials for lithium-ion battery: synergistic effect of doping and compositing," *Journal of Power Sources*, vol. 248, pp. 1034–1041, 2014.

[20] X. Guo, C. Wang, M. Chen, J. Wang, and J. Zheng, "Carbon coating of $Li_4Ti_5O_{12}$ using amphiphilic carbonaceous material for improvement of lithium-ion battery performance," *Journal of Power Sources*, vol. 214, pp. 107–112, 2012.

[21] W. Wang, Y. Guo, L. Liu, S. Wang, X. Yang, and H. Guo, "Gold coating for a high performance $Li_4Ti_5O_{12}$ nanorod aggregates anode in lithium-ion batteries," *Journal of Power Sources*, vol. 245, pp. 624–629, 2014.

[22] T. Yuan, W.-T. Li, W. Zhang et al., "One-pot spray-dried graphene sheets-encapsulated nano-$Li_4Ti_5O_{12}$ microspheres for a hybrid BatCap system," *Industrial & Engineering Chemistry Research*, vol. 53, no. 27, pp. 10849–10857, 2014.

[23] Q. Cheng, S. Tang, J. Liang et al., "High rate performance of the carbon encapsulated $Li_4Ti_5O_{12}$ for lithium ion battery," *Results in Physics*, vol. 7, pp. 810–812, 2017.

[24] Q. Zhang and X. Li, "Recent developments in the doped-$Li_4Ti_5O_{12}$ anode materials of lithium-ion batteries for improving the rate capability," *International Journal of Electrochemical Science*, vol. 8, pp. 6449–6456, 2013.

[25] G. Xie, J. Ni, X. Liao, and L. Gao, "Filter paper templated synthesis of chain-structured $Li_4Ti_5O_{12}$/C composite for Li-ion batteries," *Materials Letters*, vol. 78, pp. 177–179, 2012.

[26] Q. Zhang, C. Zhang, B. Li, S. Kang, X. Li, and Y. Wang, "Preparation and electrochemical properties of Ca-doped $Li_4Ti_5O_{12}$ as anode materials in lithium-ion battery," *Electrochimica Acta*, vol. 98, pp. 146–152, 2013.

[27] J. H. Kim, D. Bhattacharjya, and J.-S. Yu, "Synthesis of hollow TiO_2@N-doped carbon with enhanced electrochemical capacitance by an in situ hydrothermal process using hexamethylenetetramine," *Journal of Materials Chemistry A*, vol. 2, no. 29, pp. 11472–11479, 2014.

[28] T.-F. Yi, H. Liu, Y.-R. Zhu, L.-J. Jiang, Y. Xie, and R.-S. Zhu, "Improving the high rate performance of $Li_4Ti_5O_{12}$ through divalent zinc substitution," *Journal of Power Sources*, vol. 215, pp. 258–265, 2012.

[29] T. F. Yi, S. Y. Yang, and Y. Xie, "Recent advances of $Li_4Ti_5O_{12}$ as a promising next generation anode material for high power lithium-ion batteries," *Journal of Materials Chemistry A*, vol. 3, no. 11, pp. 5750–5777, 2015.

[30] Y. Ma, B. Ding, G. Ji, and J. Y. Lee, "Carbon-encapsulated F-doped $Li_4Ti_5O_{12}$ as a high rate anode material for Li^+ batteries," *ACS Nano*, vol. 7, no. 12, pp. 10870–10878, 2013.

[31] J. Zhao, C. Liu, H. Deng et al., "In-situ catalytic growth carbon nanotubes from metal organic frameworks for high performance lithium-sulfur batteries," *Materials Today Energy*, vol. 8, pp. 134–142, 2018.

[32] K. S. Park, A. Benayad, D. J. Kang, and S. G. Doo, "Nitridation-driven conductive $Li_4Ti_5O_{12}$ for lithium ion batteries," *Journal of the American Chemical Society*, vol. 130, no. 45, pp. 14930-14931, 2008.